



## Thermoelectric characterization of ion beam sputtered $\text{Sb}_2\text{Te}_3$ thin films

Ping Fan\*, Zhuang-Hao Zheng, Guang-Xing Liang, Dong-Ping Zhang, Xing-Min Cai

College of Physical Science and Technology, Institute of Thin Film Physics and Applications, Shenzhen Key Laboratory of Sensor Technology, Shenzhen University, 518060, China

### ARTICLE INFO

#### Article history:

Received 10 February 2010

Received in revised form 3 June 2010

Accepted 10 June 2010

Available online 18 June 2010

#### Keywords:

Ion beam sputtering

$\text{Sb}_2\text{Te}_3$  thin films

Thermoelectric material

Heat treatment

### ABSTRACT

Ion beam sputtering was used to deposit  $\text{Sb}_2\text{Te}_3$  thin films on BK7 glass substrates at room temperature. The effect of annealing on the thermoelectric properties of the  $\text{Sb}_2\text{Te}_3$  thin films was investigated. After the stoichiometric films were annealed at 100 °C to 400 °C for one hour, the Seebeck coefficient decreases from  $190 \mu\text{V K}^{-1}$  to  $106 \mu\text{V K}^{-1}$ , and the conductivity increases from  $1.1 \times 10^2 \text{ S cm}^{-1}$  to  $2.01 \times 10^3 \text{ S cm}^{-1}$ . The Power Factor is enhanced greatly from  $0.40 \times 10^{-3} \text{ W m}^{-1} \text{ K}^{-2}$  to  $2.26 \times 10^{-3} \text{ W m}^{-1} \text{ K}^{-2}$  after annealing at 400 °C. The positive Seebeck coefficient  $\alpha$  suggests the films to be p-type. X-ray diffraction (XRD) shows that the major diffraction peaks of the films match those of  $\text{Sb}_2\text{Te}_3$  and high crystalline films are achieved after annealing. These results indicate that high-quality  $\text{Sb}_2\text{Te}_3$  thin films are achieved and annealing greatly improves the thermoelectric properties of the films.

© 2010 Elsevier B.V. All rights reserved.

### 1. Introduction

Thermoelectric techniques are widely employed in solid-state coolers, power generators, sensors and optical storage systems [1–4]. V–VI compound semiconductors, with  $\text{A}_2\text{B}_3$ -type, are well-established room-temperature thermoelectric materials because of their excellent thermoelectric properties. Both theoretical [5] and experimental [6,7] work show that low-dimensional alloys have higher figure of merit (ZT) due to their stronger quantum confinement effect.

Antimony telluride ( $\text{Sb}_2\text{Te}_3$ ) is an important V–VI thermoelectric material at room-temperature due to its excellent thermoelectric properties, narrow-band gap and high figure of merit (ZT) value [8,9]. A lot of techniques, including co-evaporation [10], electrochemical deposition [11] and chemical-vapor deposition [12] have been used to grow  $\text{Sb}_2\text{Te}_3$  thin films. However, both the Seebeck coefficients ( $\alpha$ ) and conductivity ( $\sigma$ ) of the films are found to be worse than those of bulk material. This is mainly due to the difficulty in controlling the composition. The vapor pressure of Te is so high compared with that of Sb and the re-evaporation of Te is not in favor of the formation of  $\text{Sb}_2\text{Te}_3$ . Precise control of the composition is therefore particularly important in achieving good thermoelectric properties of  $\text{Sb}_2\text{Te}_3$  thin films. Actually, ion beam sputtering deposition (IBSD) is a very attractive technique since it combines a high deposition rate with a great versatility in the deposition of films by adjusting the target composition and controlling the sputtering energy. In addition, preparing  $\text{Sb}_2\text{Te}_3$  thin films by ion beam sputtering deposition is rarely reported.

In this paper, ion beam sputtering was used to deposit  $\text{Sb}_2\text{Te}_3$  thermoelectric thin films at room temperature. Instead of using an alloy target, the target was made of fan-shaped Sb and Te plates. This kind of target provides the convenience and efficiency in adjusting the Sb/Te composition ratio by changing the plate areas. Annealing on the thermoelectric properties of the films was then investigated.

### 2. Experimental details

$\text{Sb}_2\text{Te}_3$  thin films were deposited on BK7 glass substrates at room temperature by IBSD in argon ambience. The incident angle of the argon ion beam onto the target was about 45°. The distance between the central point of the target and the substrate is about 100 mm and the whole target area is 110 mm × 110 mm. The target was made of fan-shaped high purity Sb (99.99%) and Te (99.99%) plates. The Sb/Te ratio was controlled by adjusting the ratio of the corresponding plate areas. The chamber was pumped to a base pressure of  $7.0 \times 10^{-4}$  Pa before the introduction of Ar gas and the work pressure was maintained at  $6.1 \times 10^{-2}$  Pa. The substrates were ultrasonically cleaned in acetone and alcohol for 10 min respectively. Before depositing Sb/Te films, a 15-min sputter cleaning process was performed to remove the contaminants on the target surfaces. A Plasma voltage of 700 V and a beam current of 10 mA were used for sputtering. Samples were deposited at room temperature and the deposition time was 60 min. The film thickness was over 500 nm. In order to improve the properties of the films, more samples were prepared. These samples were then annealed at 100 °C, 200 °C, 300 °C and 400 °C for one hour in the vacuum chamber, respectively. The chamber pressure for the annealing was less than  $8.0 \times 10^{-4}$  Pa. The influence of the annealing temperature on the properties was investigated.

The composition ratio of the  $\text{Sb}_2\text{Te}_3$  thin films was determined by using an energy dispersive X-ray spectroscopy microanalysis system (EDS, Hitachi S-3400N(II)). The film thickness was obtained by using a DEKTAK<sup>3</sup> ST surface-profile measurement system. The structure of the films was studied by X-Ray diffraction (XRD, BRUKER-D8-ADVANCE) with Cu  $\text{K}\alpha$  radiation ( $\lambda = 0.15406$  nm). The electrical properties, including conductivity ( $\sigma$ ), carrier concentration ( $p$ ) and carrier mobility ( $\mu$ ) of the films were tested at room temperature by Hall coefficient measurement (ET9000). The Seebeck coefficient ( $\alpha$ ) was measured by Seebeck coefficient measurement system.

\* Corresponding author. Tel.: +86 755 26536021; fax: +86 755 26536021.  
E-mail address: [fanping@szu.edu.cn](mailto:fanping@szu.edu.cn) (P. Fan).

**Table 1**

The atomic ratio of Sb to Te and thermoelectric results of the as-deposited sample.

$R_{\text{ato}}$	$\alpha$ ( $\mu\text{V K}^{-1}$ )	$\sigma$ ( $\times 10^2 \text{ S cm}^{-1}$ )	$p$ ( $10^{23} \text{ cm}^{-3}$ )	$\mu$ ( $\text{cm}^2 \text{ V}^{-1} \text{ s}^{-1}$ )	PF ( $\text{W m}^{-1} \text{ K}^{-2}$ )
0.65	190	1.1	0.35	1.85	0.40

The Power Factor (PF), one of the important thermoelectric parameters which determines the performance of the thermoelectric energy converters, was calculated using Eq. (1) (where  $\alpha$  is the Seebeck coefficient in  $\mu\text{V K}^{-1}$  and  $\sigma$  is the conductivity in  $\text{S cm}^{-1}$ ). The conductivity, carrier concentration and mobility obey Eq. (2) (where  $p$  is the carrier concentration in  $\text{cm}^{-3}$ ,  $\mu$  is the carrier mobility in  $\text{cm}^2 \text{ V}^{-1} \text{ s}^{-1}$  and  $e$  is the charge of an electron).

$$\text{PF} = \alpha^2 \sigma \quad (1)$$

$$\sigma = pe\mu \quad (2)$$

### 3. Results and discussion

The EDS and thermoelectric measurement results were listed in Table 1 where  $R_{\text{ato}}$  is the atomic ratio of Sb to Te. The Power Factor is obtained from Eq. (1). From Table 1, it can be found that the atomic ratio of Sb to Te is around 2:3. The obtained film is therefore stoichiometric. The positive Seebeck coefficient  $\alpha$  implies that all the films are p-type. The stoichiometric film has a Power Factor of  $0.40 \times 10^{-3} \text{ W m}^{-1} \text{ K}^{-2}$ , a high conductivity of  $1.1 \times 10^2 \text{ S cm}^{-1}$  and a moderate Seebeck coefficient of  $190 \mu\text{V K}^{-1}$ .

The Seebeck coefficient of our samples approaches that of  $\text{Sb}_2\text{Te}_3$  thin films, while the Power Factor and conductivity are much smaller than those of  $\text{Sb}_2\text{Te}_3$  thin films reported by others [13–16]. The poor electric properties might be due to the poor crystalline quality since room temperature deposition usually results in poor crystallization. To study how annealing can affect the properties of the films, more samples were prepared at the same condition with this sample. These samples were then annealed at  $100^\circ\text{C}$ ,  $200^\circ\text{C}$ ,  $300^\circ\text{C}$  and  $400^\circ\text{C}$  for one hour in the vacuum chamber, respectively.

Fig. 1 shows the Seebeck coefficient and conductivity of these films as a function of the annealing temperature. For comparison, the as-deposited sample was considered to be annealed at room temperature and its properties were included in all the Figures. It can be found that the Seebeck coefficient decreases from  $190 \mu\text{V K}^{-1}$  to  $106 \mu\text{V K}^{-1}$  and the conductivity increases from  $1.1 \times 10^2 \text{ S cm}^{-1}$  to  $2.01 \times 10^3 \text{ S cm}^{-1}$ , as the temperature increases from room temperature to  $400^\circ\text{C}$ . The decrease of the Seebeck coefficient is mainly due to the evaporation of Te. The evaporation of Te during annealing can result in the loss of Te in the film and hence decrease the Seebeck coefficient. The decrease of the See-

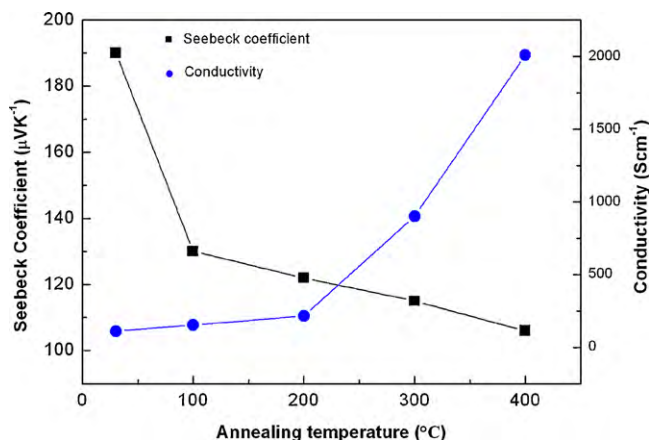
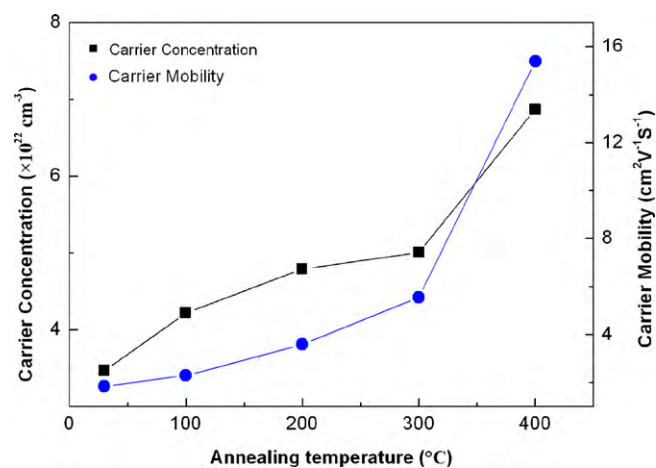


**Fig. 1.** The Seebeck coefficients and conductivities of the as-deposited and annealed samples. The as-deposited sample was considered to be annealed at room temperature. The annealing temperatures of other samples were  $100$ – $400^\circ\text{C}$ .

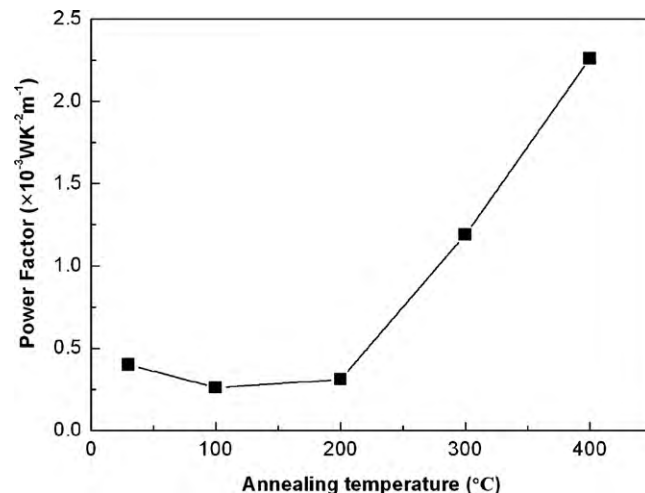
beck coefficient might also be due to oxidation after annealing at high temperature. The conductivity has an extremely high value when annealed at  $400^\circ\text{C}$ .

Fig. 2 shows the carrier concentration and mobility of the  $\text{Sb}_2\text{Te}_3$  thin films as a function of annealing temperature. The carrier concentration and mobility are near those of bulk  $\text{Sb}_2\text{Te}_3$  material. This indicates that the films have good electric properties. As can be seen from Eq. (2), the carrier concentration and mobility determine the conductivity. The carrier concentration and carrier mobility increase greatly when the annealing temperature is over  $300^\circ\text{C}$ . Thus, the change of the conductivity is much faster in the range of  $300$ – $400^\circ\text{C}$  than that in the range of room temperature to  $200^\circ\text{C}$ .

The Power Factors of all the samples are presented in Fig. 3. As is shown in Fig. 3, the Power Factors increase from  $0.40 \times 10^{-3} \text{ W m}^{-1} \text{ K}^{-2}$  to  $2.26 \times 10^{-3} \text{ W m}^{-1} \text{ K}^{-2}$  as the temperature increases to  $400^\circ\text{C}$ . Though the sample annealed at  $400^\circ\text{C}$  has a small Seebeck coefficient of  $106 \mu\text{V K}^{-1}$ , it has a very high conductivity and PF, which implies that annealing at  $400^\circ\text{C}$  has an obvious effect on the film. As can be seen from Fig. 1 to Fig. 3, the



**Fig. 2.** The carrier concentrations and mobilities of the as-deposited and annealed samples.



**Fig. 3.** The Power Factors of the as-deposited and annealed samples.

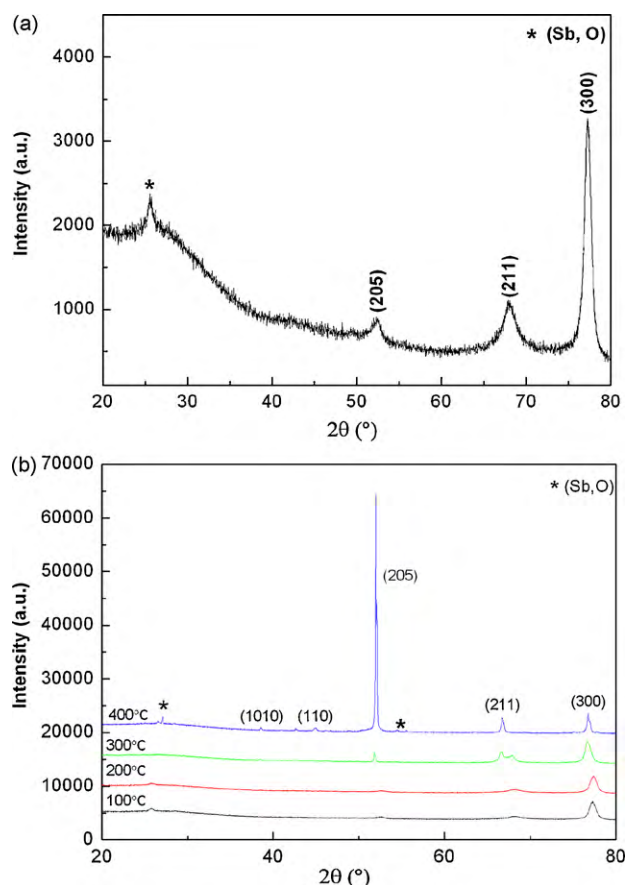


**Fig. 4.** (a) XRD pattern of the as-deposited sample; (b) XRD patterns of the samples annealed at 100 °C, 200 °C, 300 °C and 400 °C. The annealing temperature is labeled right above the corresponding curve.

conductivity, carrier concentration, carrier mobility and PF of the films increase with the increase of the annealing temperature. This reveals that annealing can improve the thermoelectric properties of the films. This might be due to the improvement of crystalline quality.

Fig. 4 shows the XRD patterns of all the samples. The XRD pattern of the as-deposited film which has the best PF is shown in Fig. 4(a). Three major diffraction peaks located at 52.67°, 67.73° and 77.37° are observed and they are indexed as the reflection from the (205), (211) and (300) planes of  $\text{Sb}_2\text{Te}_3$ . This result demonstrates the samples are  $\text{Sb}_2\text{Te}_3$  thin films with a hexagonal structure belonging to the  $R\bar{3}m$  space group [14–23]. However, the intensity of the peaks related to  $\text{Sb}_2\text{Te}_3$  is small. In addition, a peak located at 25° is also observed and this peak is labeled as (Sb, O). It is due to oxides such as SbO,  $\text{Sb}_2\text{O}_5$ ,  $\text{SbO}_3$ . Room temperature deposition usually results in poor crystallization and many defects. These defects will increase the interface scattering, etc. The electrical properties of stoichiometric  $\text{Sb}_2\text{Te}_3$  thin films will therefore be weakened. Fig. 4(b) shows the XRD patterns of the films annealed at 100 °C, 200 °C, 300 °C and 400 °C. After annealing, the samples are still hexagonal. With the increase of annealing temperature, the intensity of the peaks related to  $\text{Sb}_2\text{Te}_3$  is greatly enhanced, while the FWHM of these peaks is lowered. At higher temperature, the peaks related to  $\text{Sb}_2\text{Te}_3$  are slightly shifted to smaller angles. This could be related to the reduction of the defects and thermal stress. The diffraction peaks related to some (Sb, O) impurity are still observed clearly. It is worth noting that the XRD pattern of the sample annealed at 400 °C is quite different from others. In

the XRD pattern of this sample, peaks related to  $\text{Sb}_2\text{Te}_3$  (1010) and  $\text{Sb}_2\text{Te}_3$  (110) can be observed. In addition, the intensity of the peak labeled as (205) is the strongest and the FWHM of this peak is much lower than those of others. Though diffraction peaks related to some (Sb, O) impurity are still observed at 400 °C, their intensities are much smaller than those peaks related to  $\text{Sb}_2\text{Te}_3$ . This indicates that  $\text{Sb}_2\text{Te}_3$  is the dominant phase even after annealing at 400 °C. From the XRD results, it can be concluded that  $\text{Sb}_2\text{Te}_3$  thin films of high crystalline quality are obtained after annealing. By improving the crystalline quality, the defects are reduced and interface scattering, etc. is also reduced, which will lead to the improvement of the electrical properties.

#### 4. Conclusions

$\text{Sb}_2\text{Te}_3$  thin film was obtained by IBS. It is very convenient to prepare stoichiometric films by IBS. The films prepared by IBS have good reproducibility. EDS shows that the stoichiometric  $\text{Sb}_2\text{Te}_3$  thin film can be obtained by changing the area ratio of Sb plate to Te plate. Hall and Seebeck measurement show that stoichiometric films have better thermoelectric properties and nonstoichiometric films have poor thermoelectric properties. XRD shows that the film has a hexagonal structure. The crystalline quality and thermoelectric properties are improved after annealing. The Seebeck coefficient decreases from  $190 \mu\text{V K}^{-1}$  to  $106 \mu\text{V K}^{-1}$  and the conductivity increases from  $1.1 \times 10^2 \text{ S cm}^{-1}$  to  $2.01 \times 10^3 \text{ S cm}^{-1}$  after annealing. The best film has a maximum Power Factor of  $2.26 \times 10^{-3} \text{ W m}^{-1} \text{ K}^{-2}$ . These results show that high quality  $\text{Sb}_2\text{Te}_3$  thin films can be prepared by IBS and annealing in the vacuum can further improve their thermoelectric properties.

#### Acknowledgments

The work was supported by Open Funding Projects of Shenzhen Key Laboratory of Sensor Technology (Project No.: SST200901) and the Project of the Bureau of Science and Technology, Nanshan District, Shenzhen (No. 2009035).

#### References

- [1] J.P. Heremans, V. Jovovic, E.S. Toberer, A. Saramat, K. Kurosaki, A. Charoenphakdee, S. Yamanaka, G.J. Snyder, *Science* 321 (2008) 554.
- [2] L.E. Bell, *Science* 321 (2008) 1457.
- [3] Y.L. Li, J. Jiang, G.J. Xu, W. Li, L.M. Zhou, Y. Li, P. Cui, *J. Alloys Compd.* 480 (2009) 954.
- [4] M. Chitroub, F. Besse, H. Scherrer, *J. Alloys Compd.* 467 (2009) 31.
- [5] L.D. Hicks, M.S. Dresslhaus, *Phys. Rev. B* 47 (1993) 16631.
- [6] C.F. Wang, Q. Wang, L.D. Chen, X.C. Xu, Q. Yao, *Electrochim. Solid-State Lett.* 9 (2006) C147.
- [7] F. Volklin, V. Baier, U. Dillner, E. Kessler, *Thin Solid Films* 187 (1990) 253.
- [8] A. Boyer, E. Cissé, *Mater. Sci. Eng. B* 13 (1992) 103.
- [9] A.M. Farid, H.E. Atiyia, N.A. Hegab, *Vacuum* 80 (2005) 284.
- [10] L.M. Goncalves, P. Alpuim, G. Min, D.M. Rowe, C. Couto, J.H. Correia, *Vacuum* 82 (2008) 1499.
- [11] S.K. Lim, M.Y. Kim, T.S. Oh, *Thin Solid Films* 517 (2009) 4199.
- [12] İ.Y. Erdoğan, Ü. Demir, *J. Electroanal. Chem.* 633 (2009) 253.
- [13] A. Pattamatta, C.K. Madnia, *Int. J. Heat Mass Transfer* 52 (2009) 860.
- [14] D. Pinisetty, R.V. Devireddy, *Acta Mater.* 58 (2010) 570.
- [15] K. Park, F. Xiao, B.Y. Yoo, Y. Rheem, N.V. Myung, *J. Alloys Compd.* 485 (2009) 362.
- [16] H. Noro, K. Sato, H. Kagechika, *J. Appl. Phys.* 73 (1993) 1252.
- [17] H.L. Zou, D.M. Rowe, G. Min, *J. Cryst. Growth* 222 (2001) 82.
- [18] N.S. Patil, A.M. Sargar, S.R. Mane, P.N. Bhosale, *Mater. Chem. Phys.* 115 (2008) 47.
- [19] J.L. Yu, B. Liu, T. Zhang, Z.T. Song, S.L. Feng, B. Chen, *Appl. Surf. Sci.* 253 (2007) 6125.
- [20] Q.L. Yuan, Q.L. Nie, D.X. Huo, *Curr. Appl. Phys.* 9 (2009) 224.
- [21] F. Xiao, C. Hangarter, B. Yoo, Y. Rheem, K.H. Lee, N.V. Myung, *Electrochim. Acta* 53 (2008) 8103.
- [22] J.P. Carmo, L.M. Goncalves, J.H. Correia, *Electron. Lett.* 45 (2009) 803.
- [23] C.N. Liao, L.C. Wu, J.S. Lee, *J. Alloys Compd.* 490 (2010) 468.